

Enhanced Quantum State Transfer via Feedforward Cancellation of Optical Phase Noise

Benjamin P. Maddox¹, Jonathan M. Mortlock¹, Tom R. Hepworth¹, Adarsh P. Raghuram¹, Philip D. Gregory¹, Alexander Guttridge¹, and Simon L. Cornish^{1*}

Department of Physics, Durham University, South Road, Durham DH1 3LE, United Kingdom

 (Received 16 July 2024; revised 11 October 2024; accepted 18 November 2024; published 18 December 2024)

Many experimental platforms for quantum science depend on state control via laser fields. Frequently, however, the control fidelity is limited by optical phase noise. This is exacerbated in stabilized laser systems where high-frequency phase noise is an unavoidable consequence of feedback. Here we implement an optical feedforward technique to suppress laser phase noise in the stimulated Raman adiabatic passage state transfer of ultracold RbCs molecules, across 114 THz, from a weakly bound Feshbach state to the rovibrational ground state. By performing over 100 state transfers on single molecules, we measure a significantly enhanced transfer efficiency of 98.7(1)% limited only by available laser intensity.

DOI: [10.1103/PhysRevLett.133.253202](https://doi.org/10.1103/PhysRevLett.133.253202)

Robust control of quantum states with optical fields is vital in many areas of modern physics. Depending on the platform, this can be achieved with one-photon or two-photon driving fields to perform both single-qubit and entangling operations [1–3]. Control fidelities can be enhanced by using pulse shaping schemes [4]. One widely used technique is stimulated Raman adiabatic passage (STIRAP) [5,6], which enables the transfer of population between two discrete states via coupling to an intermediate state. Notable advantages of STIRAP are that it is immune to loss through spontaneous emission from the intermediate state, and it is relatively insensitive to noise in experimental conditions such as laser intensity [6]. This has led to STIRAP finding important applications in superconducting circuits [7], trapped ions [8], nitrogen-vacancy centers [9], optomechanical resonators [10], optical waveguides [11], and ultracold molecule synthesis [12].

Despite being less sensitive to laser amplitude noise, STIRAP is inherently sensitive to fast laser phase noise as it relies on the adiabatic evolution of a dark state [6,13]. To minimize phase noise, lasers with narrow linewidths are required. This is commonly achieved by actively stabilizing the frequency of the light to a stable reference such as an optical cavity. This process reduces phase noise at frequencies within the bandwidth of the feedback loop, but can also introduce additional noise at higher frequencies. This high-frequency phase noise is colloquially known as the *servo*

bump. As is generally the case in optical quantum control [14], STIRAP is most affected by phase noise at frequencies comparable to the Rabi frequencies of the driving fields [13]. In many experiments, the servo bump and the driving Rabi frequency are unavoidably close together making this a challenge for high-fidelity control.

Filtering out the servo bumps may be achieved by passing the light through one or more additional optical cavities [2,15–18]. This technique is effective, but the filtering is accompanied by a large loss in optical power. A recently reported technique based on feedforward noise cancellation has demonstrated a reduction in optical phase noise without cavity filtering [19,20]. This approach measures the variation of phase in real time and then corrects the light sent to the experiment using an electro-optic modulator (EOM). This method is significantly simpler to implement and bypasses the power limitations associated with filter cavities.

Here we deploy feedforward phase-noise cancellation to significantly improve quantum state transfer, using STIRAP in ultracold molecules as a testbed for the technique. State transfer is an integral part of both the formation and detection of ground-state molecules produced by associating atoms. Efficient STIRAP is critical in applications where detection of the quantum state of individual molecules is required, for example in quantum simulation of spin models [21–27] or quantum information storage [28,29]. Improved state transfer using STIRAP would also be highly beneficial in providing increased molecule number in other experiments, for example studying strongly dipolar degenerate gases [30–33] or precision measurement of fundamental constants [34–37].

In this Letter, we demonstrate the use of feedforward (FF) to significantly improve quantum state transfer using STIRAP. Specifically, we consider the transfer of ultracold $^{87}\text{Rb}^{133}\text{Cs}$ (RbCs) molecules between a weakly bound

*Contact author: s.l.cornish@durham.ac.uk

[†]These authors contributed equally to this work.

Published by the American Physical Society under the terms of the [Creative Commons Attribution 4.0 International license](https://creativecommons.org/licenses/by/4.0/). Further distribution of this work must maintain attribution to the author(s) and the published article's title, journal citation, and DOI.

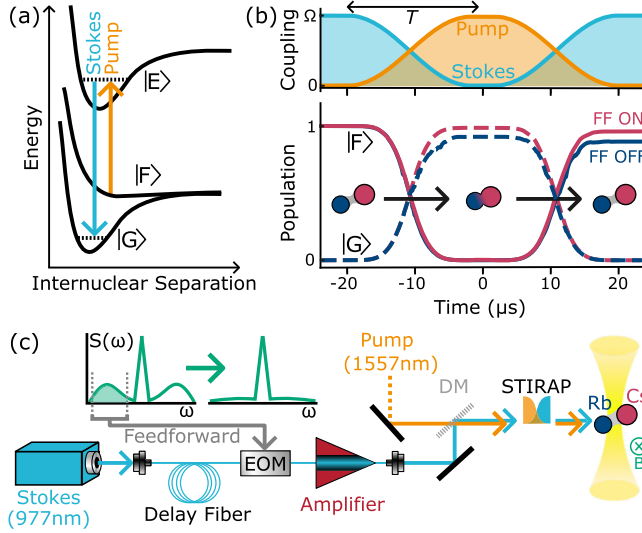


FIG. 1. STIRAP with feedforward in ultracold RbCs molecules. (a) Schematic of the STIRAP states and transitions. Molecules are initially prepared and later detected in $|F\rangle$. (b) Pulse scheme for two-way STIRAP ($N = 2$) and the associated simulated populations of $|F\rangle$ (solid lines) and $|G\rangle$ (dashed lines). The red (blue) lines indicate the expected transfer with (without) the reduction in laser phase noise from FF. (c) A simplified overview of the experiment. STIRAP of RbCs molecules in a tweezer array is achieved using two lasers, where FF noise cancellation is applied to each laser independently using a fiber EOM. The light is then amplified and combined before being sent to the molecules. The direction of the bias magnetic field (B) is orthogonal to the propagation direction of the STIRAP beams as shown.

Feshbach state and the absolute ground state spanning an energy gap of $\sim h \times 114$ THz [38]. We measure a transfer efficiency of 98.7(1)% by performing over 100 one-way transfers on a single molecule in an optical tweezer; to our knowledge this is the highest reported transfer efficiency in any ultracold polar molecule. We are able to reproduce our results by simulating the state transfer Hamiltonian with realistic laser phase noise and magnetic field instability based on independent measurements in the experiment. The model shows that our current efficiency is only limited by the available laser power, and efficiencies approaching 99.9% are possible with realistic laser intensities.

Using STIRAP as the state transfer process for preparation and readout of ultracold molecules is generic to all species formed from ultracold atoms [39–52]. Molecules are prepared in a weakly bound *Feshbach* state $|F\rangle$, which is coupled in a Λ scheme to the target ground state $|G\rangle$, via a short-lived electronically excited state $|E\rangle$. We name the laser coupling to $|F\rangle$ *pump* and that coupling to $|G\rangle$ *Stokes*, as illustrated in Fig. 1(a). With the molecules prepared in $|F\rangle$, pulsing on the off-resonant Stokes laser first initializes the system in the dark state $|D\rangle = \cos\theta|F\rangle - \sin\theta|G\rangle$. Here, $\theta = \arctan(\Omega_P/\Omega_S)$ is the mixing angle which depends on the ratio of the pump Rabi frequency Ω_P

and Stokes Rabi frequency Ω_S . Smoothly ramping down Ω_S while ramping up Ω_P preserves this dark state; this coherently transfers the molecules from $|F\rangle \rightarrow |G\rangle$, as shown in Fig. 1(b), without populating $|E\rangle$.

Lossless transfer requires extinguishing the matrix element that couples the dark state to the bright state [53]. Specifically, this requires $[2i\dot{\theta} - (\phi_S - \phi_P + \delta) \sin 2\theta] \rightarrow 0$ where δ is the two-photon detuning, and ϕ_S, ϕ_P represent the phase noise of each laser. Each term sets a timescale for the evolution of the system, and based on the theory outlined in [13,53] the transfer efficiency η becomes dependent on the pulse duration T . When the peak Rabi frequencies of the pump and Stokes fields are balanced ($\Omega_P = \Omega_S = \Omega$), the overall efficiency after repeating the transfer N times is

$$\eta(T, N) = \exp\left(-\frac{\tau_{\text{adi}}}{T} - \frac{T}{\tau_{\text{deph}}}\right)^N. \quad (1)$$

Here, $\tau_{\text{adi}} \equiv \pi^2\gamma/\Omega^2$ is the timescale of adiabaticity with γ being the decay rate from $|E\rangle$ and τ_{deph} is the dephasing timescale, which includes the effect of laser phase noise and any other noise source that causes detuning between the two lasers. The maximum efficiency achievable is equal to $\eta(T') = \exp(-2\sqrt{\tau_{\text{adi}}/\tau_{\text{deph}}})$ which occurs for a pulse time $T' = \sqrt{\tau_{\text{adi}} \times \tau_{\text{deph}}}$. The peak efficiency approaches unity as $\tau_{\text{adi}} \rightarrow 0$ or $\tau_{\text{deph}} \rightarrow \infty$.

Decreasing τ_{adi} requires increasing Ω by using higher laser intensities. However, this also changes the frequency components of the phase noise which contribute most to τ_{deph} . This presents an experimental challenge for STIRAP in molecule formation, where the large (typically, ~ 100 THz) energy gap from Feshbach state to rovibrational ground state is bridged with two independent lasers stabilized to optical cavities or frequency combs. The stabilization typically produces a servo bump at the \sim MHz scale which tends to coincide with the STIRAP Rabi frequency. This problem of sensitivity to high-frequency laser phase noise is generic to many platforms where stabilized lasers are used for quantum control, notably trapped ions [54] and Rydberg atoms [55,56]. In this regime, improving state transfer efficiency requires suppression of phase noise at frequencies above the bandwidth of the feedback loop.

We use FF to cancel high-frequency noise with relatively minor modifications to our pre-existing setup. Our STIRAP laser system is based on two external cavity diode lasers (ECDLs), each seeding its own fibre amplifier. The Stokes laser operates at 977 nm and the pump at 1557 nm. Both lasers are frequency-stabilized in the standard configuration, using an offset Pound-Drever-Hall (PDH) lock to a high-finesse optical cavity [57,58]. To perform FF, we add a time-delay fiber and fiber EOM between each ECDL and their respective fiber amplifier as shown in Fig. 1(d). We take the error signal from the PDH lock, invert and amplify that signal, and then feed that signal to the EOM.

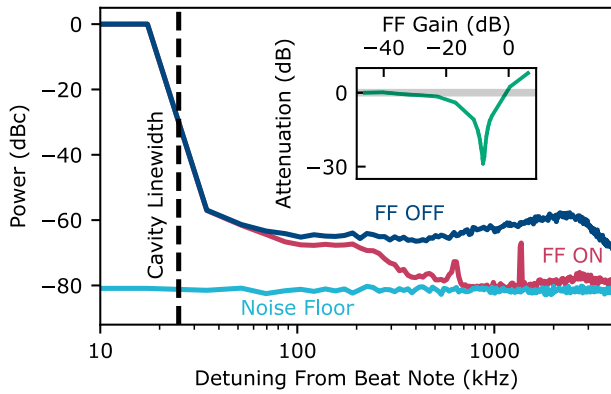


FIG. 2. Self-heterodyne measurement of the Stokes laser with the cavity transmission. Noise power relative to the beat note carrier is shown for feedforward off (dark blue) and feedforward on (red). We also plot the detection noise floor for reference (light blue), measured by blocking the cavity transmission. Residual spikes in the FF on spectrum are believed to originate from interference due to neighboring instruments. Inset: measured suppression of sinusoidal frequency modulation as a function of the gain of the FF amplifier, as described in the main text.

This modulates the light so that any high-frequency phase is cancelled out [19,20]. Effective cancellation relies on matching the amplitude of the modulation with the phase noise on the light. It also requires that the light and the electronic FF signal experience the same time delay between the error signal detection and the modulation [59]. Both of these requirements must be met over the whole bandwidth where noise must be cancelled. A more detailed description of the FF setup is given in the Supplemental Material [60].

To quantify the performance of FF, we perform self-heterodyne measurements of the phase noise of each laser. We overlap the laser light with light transmitted by the high-finesse cavity and detect the resulting beat note on a photodiode. Here, phase noise at frequencies above the cavity linewidth of 25 kHz can be considered to pertain exclusively to the main laser path [61]. Example measurements using the Stokes laser are shown in Fig. 2. In the absence of FF, the servo bump can be seen at ~ 2 MHz. By adding FF, we significantly reduce the magnitude of phase noise at the servo bump by ~ 20 dB such that it becomes comparable to the measurement noise floor.

When the FF is near optimal it is difficult to measure the true phase noise due to the finite background noise. Therefore to optimize the amplitude and delay of the FF signal we add an artificial phase noise peak at 1 MHz by modulating the current of the laser sinusoidally. The inset of Fig. 2 shows the suppression that we measure using this technique as a function of the gain of the inverting amplifier before the EOM (FF gain). We measure a suppression of 29 dB when the amplifier gain is optimal. We find this to be robust over time, though note it is susceptible to fluctuations in the amplitude of the cavity reflection. This problem can be addressed with an adaptive gain system [62].

We test the effect of FF on molecular state transfer using single RbCs molecules confined to an array of optical tweezers. The details of this apparatus have been described previously in [63–65]. Rb and Cs atoms in species-specific tweezers are cooled to their respective motional ground states, merged, and then associated by ramping over an interspecies Feshbach resonance at 197.1 G [66,67], and then transferred to $|G\rangle$ by STIRAP. We measure the fidelity of STIRAP as part of the overall infidelity in formation of a molecule in $|G\rangle$ from an atom pair, as explained in [65]. If there is an error in forming a molecule and an atom pair remains in the tweezer we detect this via pulling out Rb atoms with a species-specific tweezer into a separate error detection array. After the formation of the molecule, we reverse the STIRAP and magneto-association and this time separate the Rb atom into a different imaging array of Rb-specific tweezers. Thus we are able to measure the molecule recovery probability P_r as the probability of imaging Rb and Cs pairs conditioned on not imaging a Rb atom in the error detection array. The STIRAP fidelity is only one of many multiplicative factors in P_r , and so to make measurements more sensitive to STIRAP we perform multiple state transfers on the molecule before dissociation. To improve statistics we prepare arrays, and average over up to six tweezers per shot.

The STIRAP light is focused onto the molecules with waists of $72(3)$ μm for the Stokes and $63(3)$ μm for the pump. The light propagates perpendicular to the applied magnetic field that defines the quantization axis. Both lasers are linearly polarized, with the Stokes polarized perpendicular and the pump polarized parallel, to the magnetic field. We can apply up to 110 mW of Stokes light and 272 mW of pump light. By driving one-photon Rabi oscillations as in [68] we measure the individual Rabi frequencies of $\Omega_S^{\text{max}} = 1190(30)$ kHz and $\Omega_P^{\text{max}} = 1170(20)$ kHz (see Supplemental Material [60]). The intensity of each beam is modulated with acousto-optic modulators to achieve STIRAP using the \cos^2 -pulse shape.

To find the optimal pulse time, we take measurements of the molecule recovery probability after $N = 10$ while varying T as shown in Fig. 3(a). We fit the data with Eq. (1) to extract values of τ_{adi} and τ_{deph} . We find good agreement between our results and this model, with a sharp rise in probability below T' as the transfer becomes adiabatic, and then a slow decay from decoherence as T increases further. Comparing FF on and off, we see similar τ_{adi} for both cases as expected. We find $\tau_{\text{adi}} = 1.0(1)$ μs for FF on and $\tau_{\text{adi}} = 0.8(1)$ μs for FF off. In contrast, adding FF changes τ_{deph} significantly. Without FF $\tau_{\text{deph}} = 0.73(9)$ ms; however, with FF active this is increased by nearly an order of magnitude to $\tau_{\text{deph}} = 5.0(6)$ ms. This dramatic effect shows that phase noise is indeed the main limiting factor on τ_{deph} , and with FF on, the maximum transfer efficiency can peak higher.

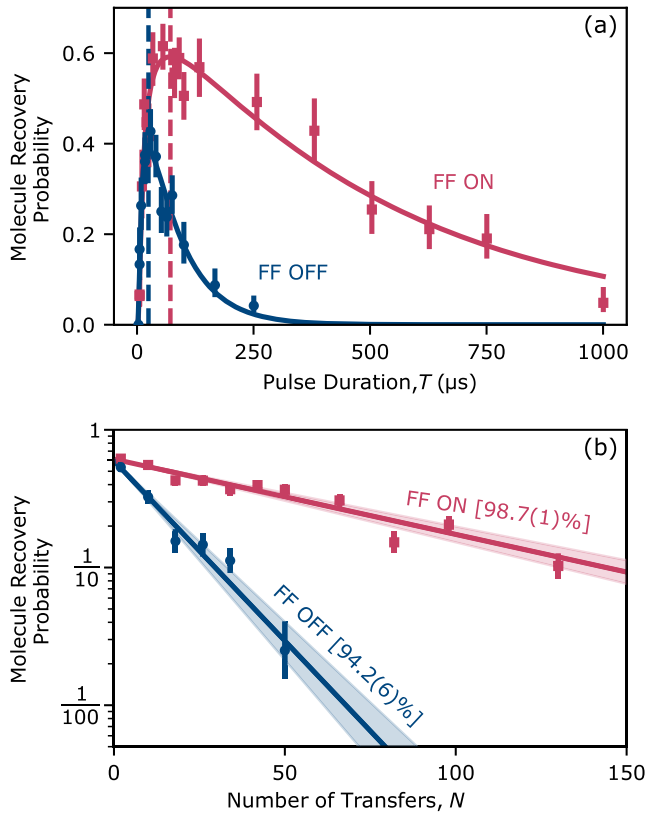


FIG. 3. Experimental results showing improved STIRAP using feedforward. (a) Molecule recovery after $N = 10$ transfers with varying STIRAP pulse duration T , for FF on (red squares) and FF off (blue circles). Solid lines show fits to the data using the model given in Eq. (1). Dashed vertical lines indicate the optimum pulse durations in each case. (b) Molecule recovery after an even number of STIRAP one-way trips, with and without FF using the optimal pulse durations shown in (a).

To more precisely determine the STIRAP efficiency, we measure the molecule recovery probability as a function of N as shown in Fig. 3(b). The transfer time is set to maximize the efficiency, such that without FF $T' = 23.85 \mu\text{s}$ and with FF $T' = 45 \mu\text{s}$. We perform a log-linear fit to the results with the gradient indicating the efficiency of each passage. The extracted efficiencies are $\eta_{\text{on}} = 98.7(1)\%$ for FF on and $\eta_{\text{off}} = 94.2(6)\%$ for FF off. These results can be expressed as a reduction in the transfer error by a factor of 4.5(5). As STIRAP efficiency is an important factor in the formation of molecules and is the dominant error in their detection, this is an important step in the quantum control of molecules. Bringing the error rate of state transfer below $\sim 1\%$ is crucial in many applications including high fidelity quantum simulation [69] and quantum information storage [70].

To understand how higher efficiencies can be achieved, we compare our results to a model of the STIRAP which accounts for the main noise contributions in our system. Our simulations are based upon the three-level model described in [53]. The laser phase noise was simulated

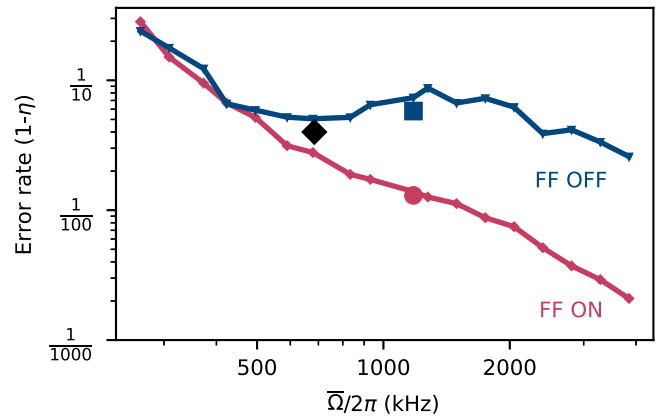


FIG. 4. Simulated error rate ($1-\eta$) of STIRAP as a function of average maximum Rabi frequency $\bar{\Omega} = (\Omega_p + \Omega_s)/2$. A red circle (blue square) marks the experimental data for FF on (off) as measured in Fig. 3(b). The measurement from our previous work in [65] is marked by a black diamond. Error bars on the experimental points are smaller than the marker size.

by extracting phase noise in angular units from the cavity-laser beat note spectra in Fig. 2 in the same manner as [71], and then initializing the noise to be the sum of sinusoids matching the spectrum amplitudes and with randomized phases. Lower frequency noise contributions are included in the model as a randomized shot-to-shot two-photon detuning. The largest contribution to this is from magnetic field noise which we estimate causes a deviation of 30 kHz. There is also a smaller contribution from the laser linewidth. We measure the linewidth of the Stokes laser to be 346(3) Hz from the half-width at half-maximum of a beat measurement between our laser and an identical but otherwise independent laser system. We assume that the linewidth of the pump and Stokes lasers are the same. We use the natural decay rate from the excited state which we have previously estimated to be $\gamma = 35(3)$ kHz [68] and neglect coupling to other states. More details of the noise model can be found in the Supplemental Material [60].

The results of our simulation are presented in Fig. 4, which shows the simulated STIRAP error rate ($1-\eta$) as a function of the average Rabi frequency $\bar{\Omega} = (\Omega_p + \Omega_s)/2$. At low Rabi frequencies, the magnetic field noise dominates over the phase noise and efficiency is gained simply by lowering τ_{adi} , with no advantage to using FF. As $\bar{\Omega}$ increases, the transfer becomes more sensitive to laser phase noise. Without FF, this causes the error rate to increase above ~ 700 kHz, tracing out the shape of the servo bump. With FF on, the error rate decreases as a function of $\bar{\Omega}$, with no apparent impact from the servo bump. We plot our measured error rates, along with those from [65] as the markers in Fig. 4. We see good agreement between the model and these experimental measurements.

Our model indicates that the efficiency can be further improved by increasing $\bar{\Omega}$, which is only limited by the available laser intensity. Extrapolating out to a reasonable

value of $\tilde{\Omega} = 4$ MHz, we can see the FF has the possibility of opening up an order of magnitude advantage in error rate compared to the FF off and approaches an error rate of 1/1000. This would require an increase in beam intensity of a factor ~ 20 . This could be easily achieved by tighter focusing of the STIRAP beams to waists sizes of 35 μm as used in [68] combined with a modest increase in the laser power to 500 and 300 mW for the pump and Stokes, respectively, which are readily available with increased amplification.

In conclusion, we have demonstrated the use of FF suppression of laser phase noise to significantly enhance state transfer efficiency. For the demanding test case of ground-state transfer using STIRAP in ultracold molecules, we achieve 98.7(1)% one-way transfer efficiency. This is the highest reported in any ultracold molecule experiment to date to our knowledge. By modeling the transfer in the presence of experimental noise, we find that the efficiency achieved is now limited by the available laser intensity. The simulation implies that efficiencies approaching 99.9% can be achieved with realistic changes to the beam waist and laser power. Our results enable the state preparation and readout of ultracold molecules with high fidelity which will be crucial for future applications of ultracold polar molecules in quantum simulation and quantum computation. Moreover, we anticipate that the techniques presented here can be readily applied to any optical quantum control scheme that is currently limited by phase noise on a stabilized laser, such as, but not restricted to, qubit operations in trapped ions [72] or Rydberg atoms [73].

Acknowledgments—We acknowledge support from the UK Engineering and Physical Sciences Research Council (EPSRC) Grants No. EP/P01058X/1 and No. EP/W00299X/1, UK Research and Innovation (UKRI) Frontier Research Grant No. EP/X023354/1, the Royal Society, and Durham University.

Data availability—The data presented in this paper are available from [74].

-
- [1] J. P. Gaebler, T. R. Tan, Y. Lin, Y. Wan, R. Bowler, A. C. Keith, S. Glancy, K. Coakley, E. Knill, D. J. Leibfried, and D. Wineland, *Phys. Rev. Lett.* **117**, 060505 (2016).
- [2] H. Levine, A. Keesling, A. Omran, H. Bernien, S. Schwartz, A. S. Zibrov, M. Endres, M. Greiner, V. Vuletić, and M. D. Lukin, *Phys. Rev. Lett.* **121**, 123603 (2018).
- [3] N. Schine, A. W. Young, W. J. Eckner, M. J. Martin, and A. M. Kaufman, *Nat. Phys.* **18**, 1067 (2022).
- [4] B. T. Torosov, B. W. Shore, and N. V. Vitanov, *Phys. Rev. A* **103**, 033110 (2021).
- [5] K. Bergmann, H. Theuer, and B. W. Shore, *Rev. Mod. Phys.* **70**, 1003 (1998).
- [6] N. V. Vitanov, A. A. Rangelov, B. W. Shore, and K. Bergmann, *Rev. Mod. Phys.* **89**, 015006 (2017).
- [7] K. S. Kumar, A. Vepsäläinen, S. Danilin, and G. S. Paraoanu, *Nat. Commun.* **7**, 10628 (2016).
- [8] D. Møller, J. L. Sørensen, J. B. Thomsen, and M. Drewsen, *Phys. Rev. A* **76**, 062321 (2007).
- [9] D. A. Golter and H. Wang, *Phys. Rev. Lett.* **112**, 116403 (2014).
- [10] V. Fedoseev, F. Luna, I. Hedgepeth, W. Löffler, and D. Bouwmeester, *Phys. Rev. Lett.* **126**, 113601 (2021).
- [11] S. Longhi, G. Della Valle, M. Ornigotti, and P. Laporta, *Phys. Rev. B* **76**, 201101(R) (2007).
- [12] C. P. Koch and M. Shapiro, *Chem. Rev.* **112**, 4928 (2012).
- [13] L. P. Yatsenko, B. W. Shore, and K. Bergmann, *Phys. Rev. A* **89**, 013831 (2014).
- [14] X. Jiang, J. Scott, M. Friesen, and M. Saffman, *Phys. Rev. A* **107**, 042611 (2023).
- [15] J. Hald and V. Ruseva, *J. Opt. Soc. Am. B* **22**, 2338 (2005).
- [16] T. Nazarova, C. Lisdat, F. Riehle, and U. Sterr, *J. Opt. Soc. Am. B* **25**, 1632 (2008).
- [17] N. Akerman, N. Navon, S. Kotler, Y. Glickman, and R. Ozeri, *New J. Phys.* **17**, 113060 (2015).
- [18] R. Bause, A. Kamijo, X.-Y. Chen, M. Duda, A. Schindewolf, I. Bloch, and X.-Y. Luo, *Phys. Rev. A* **104**, 043321 (2021).
- [19] L. Li, W. Huie, N. Chen, B. DeMarco, and J. P. Covey, *Phys. Rev. Appl.* **18**, 064005 (2022).
- [20] Y.-X. Chao, Z.-X. Hua, X.-H. Liang, Z.-P. Yue, L. You, and M. Khoon Tey, *Optica* **11**, 945 (2024).
- [21] S. L. Cornish, M. R. Tarbutt, and K. R. A. Hazzard, *Nat. Phys.* **20**, 730 (2024).
- [22] A. V. Gorshkov, S. R. Manmana, G. Chen, J. Ye, E. Demler, M. D. Lukin, and A. M. Rey, *Phys. Rev. Lett.* **107**, 115301 (2011).
- [23] L. Christakis, J. S. Rosenberg, R. Raj, S. Chi, A. Morningstar, D. A. Huse, Z. Z. Yan, and W. S. Bakr, *Nature (London)* **614**, 64 (2023).
- [24] J.-R. Li, K. Matsuda, C. Miller, A. N. Carroll, W. G. Tobias, J. S. Higgins, and J. Ye, *Nature (London)* **614**, 70 (2023).
- [25] T. Bilitewski, L. De Marco, J.-R. Li, K. Matsuda, W. G. Tobias, G. Valtolina, J. Ye, and A. M. Rey, *Phys. Rev. Lett.* **126**, 113401 (2021).
- [26] B. Yan, S. A. Moses, B. Gadway, J. P. Covey, K. R. A. Hazzard, A. M. Rey, D. S. Jin, and J. Ye, *Nature (London)* **501**, 521 (2013).
- [27] L. R. B. Picard, A. J. Park, G. E. Patenotte, S. Gebretsadkan, D. Wellnitz, A. M. Rey, and K.-K. Ni, *arXiv:2406.15345*.
- [28] J. W. Park, Z. Z. Yan, H. Loh, S. A. Will, and M. W. Zwierlein, *Science* **357**, 1 (2017).
- [29] P. D. Gregory, J. A. Blackmore, S. L. Bromley, J. M. Hutson, and S. L. Cornish, *Nat. Phys.* **17**, 1149 (2021).
- [30] A. Schindewolf, R. Bause, X.-Y. Chen, M. Duda, T. Karman, I. Bloch, and X.-Y. Luo, *Nature (London)* **607**, 677 (2022).
- [31] N. Bigagli, W. Yuan, S. Zhang, B. Bulatovic, T. Karman, I. Stevenson, and S. Will, *Nature (London)* **631**, 289 (2024).
- [32] L. De Marco, G. Valtolina, K. Matsuda, W. G. Tobias, J. P. Covey, and J. Ye, *Science* **363**, 853 (2019).
- [33] M. Schmidt, L. Lassablière, G. Quémener, and T. Langen, *Phys. Rev. Res.* **4**, 013235 (2022).

- [34] M. S. Safronova, D. Budker, D. DeMille, D. F. J. Kimball, A. Derevianko, and C. W. Clark, *Rev. Mod. Phys.* **90**, 025008 (2018).
- [35] D. DeMille, N. R. Hutzler, A. M. Rey, and T. Zelevinsky, *Nat. Phys.* **20**, 741 (2024).
- [36] C. D. Panda, B. R. O’Leary, A. D. West, J. Baron, P. W. Hess, C. Hoffman, E. Kirilov, C. B. Overstreet, E. P. West, D. DeMille, J. M. Doyle, and G. Gabrielse, *Phys. Rev. A* **93**, 052110 (2016).
- [37] J. Ye and P. Zoller, *Phys. Rev. Lett.* **132**, 190001 (2024).
- [38] P. K. Molony, A. Kumar, P. D. Gregory, R. Kliese, T. Puppe, C. R. Le Sueur, J. Aldegunde, J. M. Hutson, and S. L. Cornish, *Phys. Rev. A* **94**, 022507 (2016).
- [39] K.-K. Ni, S. Ospelkaus, M. H. G. de Miranda, A. Pe’er, B. Neyenhuis, J. J. Zirbel, S. Kotochigova, P. S. Julienne, D. S. Jin, and J. Ye, *Science* **322**, 231 (2008).
- [40] T. Takekoshi, L. Reichsöllner, A. Schindewolf, J. M. Hutson, C. R. Le Sueur, O. Dulieu, F. Ferlaino, R. Grimm, and H.-C. Nägerl, *Phys. Rev. Lett.* **113**, 205301 (2014).
- [41] P. K. Molony, P. D. Gregory, Z. Ji, B. Lu, M. P. Köppinger, C. R. Le Sueur, C. L. Blackley, J. M. Hutson, and S. L. Cornish, *Phys. Rev. Lett.* **113**, 255301 (2014).
- [42] J. W. Park, S. A. Will, and M. W. Zwiernlein, *Phys. Rev. Lett.* **114**, 205302 (2015).
- [43] M. Guo, B. Zhu, B. Lu, X. Ye, F. Wang, R. Vexiau, N. Bouloufa-Maafa, G. Quéméner, O. Dulieu, and D. Wang, *Phys. Rev. Lett.* **116**, 205303 (2016).
- [44] T. M. Rvachov, H. Son, A. T. Sommer, S. Ebadi, J. J. Park, M. W. Zwiernlein, W. Ketterle, and A. O. Jamison, *Phys. Rev. Lett.* **119**, 143001 (2017).
- [45] F. Seeßelberg, N. Buchheim, Z.-K. Lu, T. Schneider, X.-Y. Luo, E. Tiemann, I. Bloch, and C. Gohle, *Phys. Rev. A* **97**, 013405 (2018).
- [46] H. Yang, D.-C. Zhang, L. Liu, Y.-X. Liu, J. Nan, B. Zhao, and J.-W. Pan, *Science* **363**, 261 (2019).
- [47] M.-G. Hu, Y. Liu, D. D. Grimes, Y.-W. Lin, A. H. Gheorghe, R. Vexiau, N. Bouloufa-Maafa, O. Dulieu, T. Rosenband, and K.-K. Ni, *Science* **366**, 1111 (2019).
- [48] K. K. Voges, P. Gersema, M. Meyer zum Alten Borgloh, T. A. Schulze, T. Hartmann, A. Zenesini, and S. Ospelkaus, *Phys. Rev. Lett.* **125**, 083401 (2020).
- [49] W. B. Cairncross, J. T. Zhang, L. R. Picard, Y. Yu, K. Wang, and K.-K. Ni, *Phys. Rev. Lett.* **126**, 123402 (2021).
- [50] J. S. Rosenberg, L. Christakis, E. Guardado-Sanchez, Z. Z. Yan, and W. S. Bakr, *Nat. Phys.* **18**, 1062 (2022).
- [51] I. Stevenson, A. Z. Lam, N. Bigagli, C. Warner, W. Yuan, S. Zhang, and S. Will, *Phys. Rev. Lett.* **130**, 113002 (2023).
- [52] C. He, X. Nie, V. Avalos, S. Botsi, S. Kumar, A. Yang, and K. Dieckmann, *Phys. Rev. Lett.* **132**, 243401 (2024).
- [53] L. P. Yatsenko, V. I. Romanenko, B. W. Shore, and K. Bergmann, *Phys. Rev. A* **65**, 043409 (2002).
- [54] H. Nakav, R. Finkelstein, L. Peleg, N. Akerman, and R. Ozeri, *Phys. Rev. A* **107**, 042622 (2023).
- [55] T. M. Graham, M. Kwon, B. Grinkemeyer, Z. Marra, X. Jiang, M. T. Lichtman, Y. Sun, M. Ebert, and M. Saffman, *Phys. Rev. Lett.* **123**, 230501 (2019).
- [56] S. De Léséleuc, D. Barredo, V. Lienhard, A. Browaeys, and T. Lahaye, *Phys. Rev. A* **97**, 053803 (2018).
- [57] R. W. P. Drever, J. L. Hall, F. V. Kowalski, J. Hough, G. M. Ford, A. J. Munley, and H. Ward, *Appl. Phys. B* **31**, 97 (1983).
- [58] P. D. Gregory, P. K. Molony, M. P. Köppinger, A. Kumar, Z. Ji, B. Lu, A. L. Marchant, and S. L. Cornish, *New J. Phys.* **17**, 055006 (2015).
- [59] Heungjae Choi, Yongchae Jeong, Chul Dong Kim, and J. S. Kenney, *IEEE Trans. Microwave Theory Tech.* **58**, 1116 (2010).
- [60] See Supplemental Material at <http://link.aps.org/supplemental/10.1103/PhysRevLett.133.253202> for a detailed description of the feedforward laser setup, characterisation of the laser phase and intensity noise, measurements of the pump and stokes Rabi frequencies and details of the numerical simulation of the STIRAP process in the presence of noise.
- [61] F. Schmid, J. Weitenberg, T. W. Hänsch, T. Udem, and A. Ozawa, *Opt. Lett.* **44**, 2709 (2019).
- [62] Y.-X. Chao, Z.-X. Hua, X.-H. Liang, Z.-P. Yue, C. Jia, L. You, and M. K. Tey, [arXiv:2407.19642](https://arxiv.org/abs/2407.19642).
- [63] S. Spence, R. V. Brooks, D. K. Ruttley, A. Guttridge, and S. L. Cornish, *New J. Phys.* **24**, 103022 (2022).
- [64] D. K. Ruttley, A. Guttridge, S. Spence, R. C. Bird, C. R. Le Sueur, J. M. Hutson, and S. L. Cornish, *Phys. Rev. Lett.* **130**, 223401 (2023).
- [65] D. K. Ruttley, A. Guttridge, T. R. Hepworth, and S. L. Cornish, *PRX Quantum* **5**, 020333 (2024).
- [66] T. Takekoshi, M. Debatin, R. Rameshan, F. Ferlaino, R. Grimm, H.-C. Nägerl, C. R. Le Sueur, J. M. Hutson, P. S. Julienne, S. Kotochigova, and E. Tiemann, *Phys. Rev. A* **85**, 032506 (2012).
- [67] M. P. Köppinger, D. J. McCarron, D. L. Jenkin, P. K. Molony, H.-W. Cho, S. L. Cornish, C. R. L. Sueur, C. L. Blackley, and J. M. Hutson, *Phys. Rev. A* **89**, 033604 (2014).
- [68] P. K. Molony, P. D. Gregory, A. Kumar, C. R. Le Sueur, J. M. Hutson, and S. L. Cornish, *Chem. Phys. Chem.* **17**, 3811 (2016).
- [69] A. J. Daley, I. Bloch, C. Kokail, S. Flannigan, N. Pearson, M. Troyer, and P. Zoller, *Nature (London)* **607**, 667 (2022).
- [70] C. Zhang and M. R. Tarbutt, *PRX Quantum* **3**, 030340 (2022).
- [71] F. Schmid, J. Weitenberg, T. W. Hänsch, T. Udem, and A. Ozawa, *Opt. Lett.* **44**, 2709 (2019).
- [72] N. Akerman, N. Navon, S. Kotler, Y. Glickman, and R. Ozeri, *New J. Phys.* **17**, 113060 (2015).
- [73] S. De Léséleuc, D. Barredo, V. Lienhard, A. Browaeys, and T. Lahaye, *Phys. Rev. A* **97**, 053803 (2018).
- [74] B. P. Maddox, J. M. Mortlock, T. R. Hepworth, A. P. Raghuram, P. D. Gregory, A. Guttridge, and S. L. Cornish, Enhanced quantum state transfer via feedforward cancellation of optical phase noise [dataset] (2024), [10.15128/r1v979v3117](https://arxiv.org/abs/10.15128/r1v979v3117).